Conformational Behavior of Simple Furanosides Studied by Optical Rotation

JAKUB KAMINSKÝ,[1,2] IVAN RAICH,[2] KATEŘINA TOMČÁKOVÁ,[2] PETR BOUŘ[1]

[1]*Institute of Organic Chemistry and Biochemistry, Academy of Sciences, Prague, Czech Republic*

[2]*Department of Chemistry of Natural Compounds, Institute of Chemical Technology, Prague, Czech Republic*

Abstract: Experimental and theoretical specific optical rotations (OR) of anhydro, epithio, and epiminoderivatives of methyl tetrofuranosides in chloroform solutions have been compared and used as a tool for exploring their conformational behavior. The potential energy surfaces of these saccharides with reduced flexibility were examined with the density functional theory and the MP2 and CCSD(T) wavefunctions methods. Theoretical ORs were obtained by Boltzmann averaging of values calculated for local minima. Resultant rotations could be used to assess the quality of the DFT and MP2 relative conformer energies. OR values calculated for equilibrium geometries in vacuum were significantly improved when the solvent was accounted for by a polarizable continuum model and first and diagonal second OR derivatives were used for an anharmonic vibrational averaging. The DFT used as a default method reproduced the experimental data fairly well. A modified B3LYP functional containing 70% of HF exchange further improved the results. Because of the strong dependence of OR on the conformation, not only the absolute configuration could be determined, but also the conformational populations were estimated. Likewise, the predicted dependence of OR on the light wavelength well agreed with experiment. The increasing precision of the contemporary computational methods thus makes it possible to relate the specific rotation to more detailed features in molecular structure.

© 2010 Wiley Periodicals, Inc.   J Comput Chem 31: 2213–2224, 2010

Key words: optical rotation; conformational behavior; DFT; MP2; CCSD

Introduction

Furanosides with annealed three-membered heterocyclic rings are widely used as intermediates for the preparation of variously substituted derivatives in sugar chemistry.[1–3] Many of them can be biologically active. Several amino derivatives are precursors for antibiotics[4] or drugs for antiradiation treatment.[5] Large part of the therapeutics is focused on reverse transcriptase selective inhibitors. They are used as efficient antiviral agents, such as 2′,3′-dideoxy nucleosides,[6] their 3′-substituted derivatives[7] and the didehydro analogues.[8,9]

The knowledge of the structure and dynamics can facilitate synthesis of new compounds and elucidate their biological function. However, furanoses are in general very flexible and description of their conformational behavior is difficult. The conformation of the furanose ring is influenced by several contradictorily acting factors, including the anomeric[10] and gauche effects,[11] the preferred quasi-equatorial orientation of side-chains, and alternating arrangement of the substituents.

Fortunately, for the compounds studied in this work, the presence of the small ring in anhydro, epithio, or epimino derivatives causes a stiffening of the five-membered furanose ring, and molecular motion is reduced. Physical and chemical properties of such molecules are slightly different compared to more common furanoses.[12] Nevertheless, it is still not easy to determine the most likely conformations experimentally. In the past, we discussed the structural information that could be obtained

from the NMR data.[13] In this work, we concentrate on the optical rotation that can be measured more easily. As shown below, also the analysis of the OR data can be significantly enhanced by an ab initio conformational search coupled to state-of-the-art calculations of optical rotations.

Originally, optical rotation of molecules was related to the configuration of molecular chiral centers. However, it was soon realized that the measured value is often a sum including contributions from many conformers, and that the partial conformer rotations can significantly vary.[14–16] It was shown that a precise description of conformer populations is necessary to reproduce the experiment.[17] At the same time, calculated OR values can be used to verify the quality of modeled conformational space of the system and similar calculated data. When reliable computational schemes are available the system chirality expressed as OR can thus be a powerful tool for structural studies.

Such approach has become feasible since the work of Amos,[18] who performed the first ab initio calculations of the optical rotation tensors implemented at the Hartree-Fock level in a static limit for simple, non-chiral molecules. More applied ab initio calculations of OR of chiral molecules in the static limit have been published by Polavarapu.[19] Meanwhile, calculation of the frequency dependent tensor has been implemented.[20] On the example of H_2O_2 and H_2S_2, Polavarapu and Chakraborty also studied OR conformational dependence at the ab initio level.[21] Quite often, different conformers of the same molecule exhibit an opposite sign of optical rotation, e.g., as documented by Kondru et al.,[22] Pecul et al.,[15] Polavarapu et al.,[23] and Wiberg et al.[24]

Apart from the conformations, several other problems complicate practical ab initio calculations of OR. The most important ones include (1) choice of suitable theoretical level (basis set, electron correlation treatment, density functional), (2) addition of the vibrational corrections, and (3) the solvent effect. Basis set convergence studies, for example, have been performed by many groups both in the velocity and length gauge formulations using several levels (HF, DFT).[25–27] All studies indicate the importance of inclusion of diffuse functions. However, simple addition of the diffuse functions to a small basis sets may lead to unreliable results. The aug-cc-pVDZ-quality basis set was found as the smallest one that can provide rotations really comparable with experiment. The 6-311++G(2d,2p) basis produced similar, only slightly worse results. Sadlej et al. proposed polarizability-consistent basis sets[28] that for methyloxirane gave similar optical rotation as larger sets (aug-cc-pVTZ), but in a shorter time.

The most popular method nowadays for calculation of OR is the time-dependent density functional theory (TDDFT). It can involve the origin-independent formulation,[29] is economical in computational costs, and provides a good overall accuracy.[27,30] Sometimes, the TDDFT OR is overestimated as a result of a wrong estimation of excitation energies; for some systems (anionic proline) fails completely.[15] Kundrat and Autschbach have successfully shown the ability of the time-dependent DFT to reproduce the sign of the optical rotation of several aminoacids in different ionic states, as well as the dispersion of the optical rotation of such molecules. They pointed out the source of eventual errors to underestimation of the electronic excitation energies.[31,32] However, the computational costs of higher-order wavefunction electron correlation methods (MSSCF, Coupled Cluster) make them impractical for bigger and flexible molecules at present, even though their accuracy is more predictable and, in most cases, higher than for DFT.[30,33]

Addition of the vibrational corrections did not convincingly improve computational data so far, although they should be in principle included as they make a substantial part of the OR values,[34–36] similarly as for NMR shifts.[37] Likewise, a solvent can significantly change the rotation computed in vacuum. The solvent effects on the optical rotation of a broad family of molecules have successfully been studied using the polarizable continuum model (PCM),[38,39] which resulted in a better agreement with experiment. Kundrat and Autschbach has shown the simple point charge water molecules to be a computationally very efficient alternative to using quantum mechanical waters in modeling the solvent effect on a solute's chiroptical responses.[40]

With a limited success, Ruud et al. also studied the solvent influence on the zero-point vibrational corrections to optical rotation of S-methyloxirane.[36] They also found the solvent effect on the vibrational corrections to be relatively constant within the whole frequency range, contrary to the electronic (equilibrium) component which decreases in solvent with increasing frequency. In some solvents, the vibrational correction itself exceeds the equilibrium electronic part. Goldsmith et al. studied the influence of the dimer formation on the OR of pantolactone.[41] The results were compared with experimental OR as a function of the pantolactone/CCl_4 concentration. The authors found a strong effect of aggregation on OR. Beratan et al. then came up with a concept of chiral imprinting effects on the surrounding medium, which can dominate the chiroptical signatures over the response given by a simple solute's electronic structure in a specific environment.[42]

It is obvious that continuum solvent models, although they are used also in this study, provide only a part of the solvent influence. Unfortunately, more appropriate explicit cluster averaging[43,44] is too computationally demanding for our compounds. In this work, calculated optical rotation was used as a probe for the quality of modeled conformational space of a series of furanoside derivatives. Contribution of several effects on the resulting optical rotation was discussed. Calculated optical rotations were compared to available experimental values. As shown below, in spite of the adopted approximations, the computed optical rotations go along the experimental data quite well, and indicate that this property can be used to determine not only the absolute configuration, but also conformer equilibria of molecules.

Theory

The optical rotation has been measured as a rotation of the plane of a linearly polarized light when passing through the sample for a long time. Modern quantum optical rotation theory started by the work of Rosenfeld[45] in 1928. The rotation is caused by molecular polarization and both the electric and magnetic field components of the electromagnetic radiation contribute to this phenomenon. Molecular electric and magnetic molecular dipole moments ($\vec{\mu}_\alpha$ and $\vec{m}_\alpha$, respectively) in a presence of electric E_α

and magnetic B_α field (α-component, $\alpha = x, y, z$) can be written as:

$$\vec{\mu}_\alpha = \vec{\mu}_\alpha^0 + \overset{\leftrightarrow}{\alpha}_{\alpha\beta}\vec{E}_\beta + \omega^{-1}\overset{\leftrightarrow}{G}'_{\alpha\beta}\vec{B}_\beta + \ldots, \qquad (1a)$$

$$\vec{m}_\beta = \vec{m}_\beta^0 - \omega^{-1}\overset{\leftrightarrow}{G}'_{\alpha\beta}\frac{\partial\vec{E}_\alpha}{\partial t} + \ldots, \qquad (1b)$$

where $\alpha_{\alpha\beta}$ is the electric dipole-electric dipole polarizibility, $\overset{\leftrightarrow}{G}'_{\alpha\beta}$ is electric dipole-magnetic dipole polarizibility (often referred to as the optical rotation tensor), ω is the angular frequency of the incident monochromatic light; $\vec{\mu}^0$ and $\vec{m}^0$ are the static moments in the absence of an external field. Tensor $\overset{\leftrightarrow}{G}'_{\alpha\beta}$ is given by

$$\overset{\leftrightarrow}{G}'_{\alpha\beta} = \frac{-4\pi}{h}\sum_{n\neq s}\frac{\omega}{\omega_{ns}^2 - \omega^2}\text{Im}\{\langle\Psi_s^0|\hat{\mu}_\alpha|\Psi_n^0\rangle\langle\Psi_n^0|\hat{m}_\beta|\Psi_s^0\rangle\}, \qquad (2)$$

where Ψ_0 and Ψ_n are the ground and excited-state wave functions, and $\hat{\mu}_\alpha$ and $\hat{m}_\beta$ are the electric and magnetic dipole operators, respectively. The angular frequency ω_{ns} is defined from the state energies as $\omega_{ns} = (E_n^0 - E_s^0)/\hbar$. For isotropic samples (solutions) an optical rotatory parameter β can be introduced as a trace of $\overset{\leftrightarrow}{G}'_{\alpha\beta}$,

$$\beta = -\frac{1}{3\omega}\sum_\alpha\overset{\leftrightarrow}{G}'_{\alpha\alpha}. \qquad (3)$$

A specific rotation at frequency v (in cm^{-1}) is then

$$[\alpha]_v = \frac{28800\pi^2 N_A v^2}{c^2 M}[\beta(v)]_0, \qquad (4)$$

where N_A is the Avogadro's number and M molecular weight.

Vibrational averaging of optical rotation in semirigid molecules can be based on the expansion of the nuclear potential V and the rotation $[\alpha]_v$ in a Taylor series of the coordinates. In this study, the potential was expanded up to fourth powers of the normal mode coordinates Q_i as[37]

$$V = \frac{1}{2}\sum_{i=1}\omega_i^2 Q_i^2 + \frac{1}{6}\sum_{i=1}\sum_{j=1}\sum_{k=1}c_{ijk}Q_iQ_jQ_k$$
$$+ \frac{1}{24}\sum_{i=1}\sum_{j=1}\sum_{k=1}\sum_{l=1}d_{ijkl}Q_iQ_jQ_kQ_l, \qquad (5)$$

where the summations run over all modes i with harmonic frequencies ω_i. All cubic (c_{ijk}) and semidiagonal quartic (d_{iijk}) constants were considered.

Similarly, the rotation was expanded as

$$[\alpha] = [\alpha]_0 + \sum_i[\alpha]_{1,i}Q_i + \frac{1}{2}\sum_{i,j}[\alpha]_{2,ij}Q_iQ_j, \qquad (6)$$

where $[\alpha]_1$ and $[\alpha]_2$ are the first and second normal mode OR derivatives, respectively. From a vibrational function Ψ vibrationally-averaged rotations were obtained as
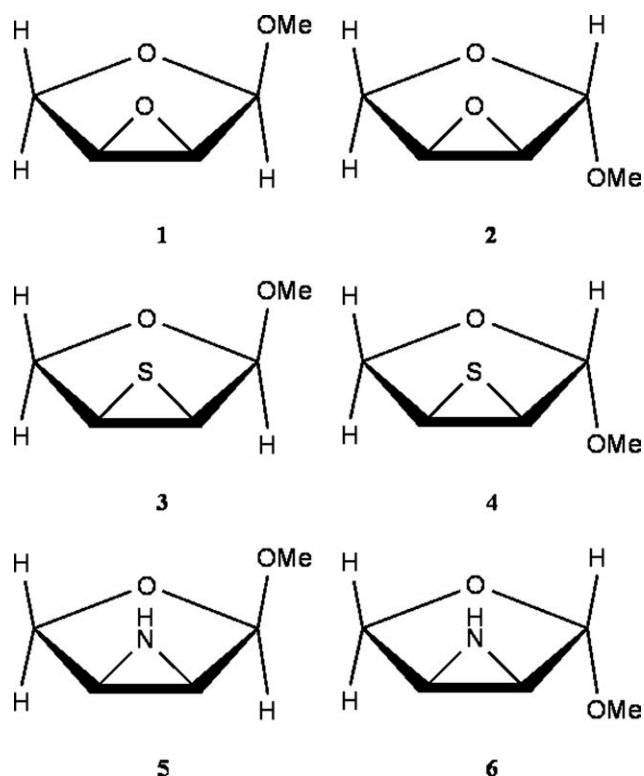

Figure 1. The studied furanoses.

$$[\alpha]_{\text{ave}} = \langle\Psi|[\alpha]|\Psi\rangle. \qquad (7)$$

The cubic and quartic force constants we obtained numerically from Hessians calculated analytically by Gaussian, for geometries displaced in normal modes. Likewise, the first and diagonal ($[\alpha]_{2,\text{ii}}$) second OR derivatives were calculated numerically. The vibrational function was obtained using the second order degeneracy-corrected perturbational calculation, using the potential in (5) and the harmonic-oscillator basis functions.[37,46] Program S4[47] interfaced to Gaussian was used for the anharmonic vibrational averaging.

Experimental

Specific rotation at the sodium D line ($\sim$589 nm) and five additional wavelengths (365, 405, 436, 546, and 633 nm) was measured in chloroform for compounds **1-6** at different concentrations, on the Autopol IV (Rudolph Research Analytical) photoelectric polarimeter.[48,49] Synthesis and NMR characteristic of the compounds were described previously.[48–50] The solvent was purchased from Aldrich.

Calculations

Even the conformationally restricted compounds **1-6** (see Fig. 1) exhibit multiple stable conformers. A relaxed potential energy surface (PES) scan was carried out for 18 (compounds **1-4**) and
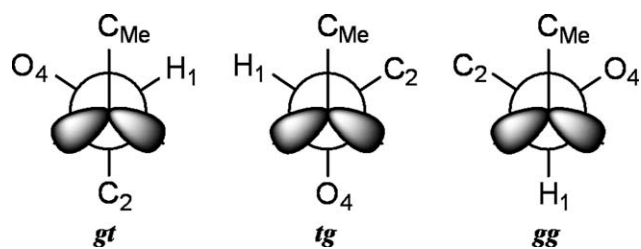
Figure 2. The notation used for the *gauche-trans* (*gt*), *trans-gauche* (*tg*) and *gauche-gauche* (*gg*) local minima of compound **1**. Analogous system was used for **2-6**.

54 (compounds **5** and **6**) starting geometries. The initial structures were constructed from two envelope conformations ^0E and E_0 and one planar structure. The puckering notation follows the Altona and Sundaralingam's pseudorotation itinerary,[51] where the envelope furanose conformer (designated as E) has four ring atoms in a plane and the remaining one above (designated by a superscript) or below (subscript). Symbol 0 denotes the ring oxygen. The scan also involved the rotation of the exocyclic C1—O1 bond with a $120°$ step and the O1—C_{OMe} bond with $180°$ step.

All structures were optimized at the B3LYP/6-311++G** level and obtained local minima were re-optimized at MP2/6-311++G**. The convergence of the minimizations was verified by calculating of harmonic vibrational frequencies. Improved estimates of relative conformational energies were obtained by single point calculations using the cc-pVnZ (n = 3–5) basis sets. The best estimate of relative MP2 energies were obtained by separately extrapolating the Hartree-Fock[52] and MP2[53] energies to the basis set limit. The chloroform solvent was modeled with the conductor-like polarizable continuum model (CPCM).[54] The CPCM bulk model is assumed to represent the chloroform quite faithfully, because specific solute-solvent interactions, such as hydrogen bonds, are rather weak. All calculations of dynamic ORs were done assuming the frequency of 589 nm corresponding to the sodium D line. Two different GGA and two hybrid DFT functionals were tested; OLYP (Handy's OPTX modification of Becke's exchange functional[55] with Lee-Yang-Parr correlation functionals[56]), PBE (The 1996 functional of Perdew, Burke, and Ernzerhof[57] with their gradient-corrected correlation functional), B3LYP (Becke 1988 exchange functional[58]) and B3PW91 (Becke's functional with Perdew-Wang 1991 correlation functionals[59]). The CCSD theory that is supposed to more precisely describe low electronic excitations was also used. Large basis sets were employed (aug-cc-pVDZ, aug-cc-PVTZ,

and aug-cc-pVQZ) to produce precise results. All ab initio calculations were performed using the Gaussian[60] and Dalton[61] programs.

For the vibrational effects all cubic and semidiagonal quartic (with two and more normal mode identical indices) force constants were obtained by a numerical differentiation of harmonic force fields. Vibrationally averaged optical rotations were obtained according to equations **6-7** where only the first ($\alpha_{1,i}$) and diagonal second ($\alpha_{2,ii}$) derivatives were considered at the B3LYP/aug-cc-pVDZ level.

Results and Discussion

Geometry Parameters

The resulting conformation of the furanose ring is in general influenced by several contradictory effects, i.e., the anomeric[10] and gauche effects,[11] the preferred quasi-equatorial orientation of side-chains, or alternating arrangement of substituents. In the case of compounds **1-6** a significant rigidity is enforced by the annealed three-membered ring. Moreover, compared to pentofuranoses, the side-chain at C4 is completely missing.

The optimizations of all starting geometries at the B3LYP level in vacuum converged to single furanose ring geometry, assigned according to the common nomenclature[51] as the envelope ^0E. In such a conformation, all carbon atoms of the furanose ring lay approximately in a plane and only the ring oxygen atom O4 is above. Three-membered ring damps the anomeric effect. Three different ^0E minima were found for all compounds **1-6** except of **2**, differing by the rotation of the methoxyl group. These minima correspond approximately to *trans-gauche* (*tg*), *gauche-trans* (*gt*) and *gauche-gauche* (*gg*) orientations at the methoxyl segment C2—C1—O1—C_{Me} (see Fig. 2).

In the case of compound **2** the *gg* conformation was not stable. Table 1 summarizes selected important structural parameters of compound **1** (parameters for other compounds are not listed here). The endo orientation seems to be the most energetically favorable position of the hydrogen atom of the —NH— group in **5** and **6**, heading above the plane of the three-membered ring toward the oxygen. A nonbonding interaction between O4 and —NH— can stabilize such a conformation and apparently slightly increases a puckering of the furanose ring if compared to **1–4**. The C2—C3 bond exhibits a shortening of about 4–9 pm compared to structurally similar tetrofuranoses or their glycosides without three-membered ring.[62] The shortening is caused by the opening of the C1—C2—C3 and C2—C3—C4 angles by about 3–6° compared to simple tetrofuranoses. Except of the

Table 1. Selected Structural Parameters of Compound 1.

Conf.	C_2—O_{23}	C_3—O_{23}	C_2—C_3—O_{23}	C_3—C_2—O_{23}	C_1—C_2—C_3—C_4	C_2—C_1—O_1—C_{Me}	C_3—C_2—C_1—O_4
gt	143	143	59.3	59.2	−0.9	177.2	11.6
tg	143	143	59.2	59.3	−0.1	80.8	9.4
gg	144	143	59.5	59.2	−1.7	−58.0	14.8

Bond lengths (in pm), bond angles, and torsion angles (in deg.) are presented for three conformers as obtained at the B3LYP/6-311++G** level. O_{23} denotes the epoxy oxygen atom.

Table 2. Relative Conformer Energy Dependence on the Basis Set.

Conf.	HF			B3LYP			MP2			
	T	Q	5	T	Q	5	T	Q	5	CBS
Compound **1**										
gt	0.0	0.0	0.0	0.0	0.0	0.0	0.0	0.0	0.0	0.0
tg	13.1	12.8	12.7	11.6	11.9	12.2	13.1	12.6	12.5	12.5
gg	1.8	2.7	2.9	0.5	1.4	1.7	1.8	−2.3	−2.0	−1.9
Compound **3**										
gt	0.0	0.0	0.0	0.0	0.0	0.0	0.0	0.0	0.0	0.0
tg	13.2	13.1	13.1	12.0	11.9	11.8	12.1	12.2	12.3	12.4
gg	9.9	10.4	10.5	6.9	7.4	7.5	4.2	4.5	4.6	4.6

Relative energies (in kJ/mol) for three local minima of compounds **1** and **3** obtained at the B3LYP, HF, and MP2 levels in vacuum, with the cc-pVnZ (n = 3, 4, 5) basis sets. The column "CBS" shows the MP2 values extrapolated to the infinite basis set limit.

methoxyl group orientation at C1, the anomers have similar geometry with a small fluctuation of the C1—O1 bond length only.

The β-anomer of the epithio derivative has the C1—O1 bond longer by 3 pm than the α-anomer. The presence of the bulky sulphur atom in **3** and **4** caused a 1 pm prolongation of C1—C2 and C3—C4 bonds compared to the epimino and anhydro derivatives. The sulphur atom also causes a deformation of the three-membered ring. Three-membered rings in **1**, **2**, **5**, and **6** form almost an ideal equilateral triangle with bond angles of about $60°$ and bond lengths of 143–148 pm, while in the epithio derivatives there is an isosceles triangle with bond angle at the sulphur atom of $47°$.

The influence of the environment on the potential energy surface was investigated with several solvents (benzene, chloroform, ethanol, and dimethylsulfoxide) characterized by their dielectric constants. The solvents caused only small differences in geometries compared to vacuum, except for compound **2**, where a new *gg* local minimum appeared. Thus three minima are predicted for all compounds in solutions.
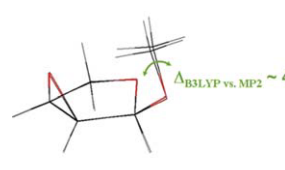
Energetics

Table 2 sums up the relative vacuum energies of conformers **1** and **3** as calculated at the HF, B3LYP, and MP2 levels and their basis set dependence. Note, that the local minima were obtained by optimizations at the B3LYP/6-311++G** level. The best relative MP2 energies can be obtained by an extrapolation to the basis set limit as reported elsewhere.[63] Table 2 thus also presents the extrapolated MP2 energies (column CBS). The DFT, as well as HF, favored the *gt* conformation in **1**, while the MP2 preferred the more folded *gg* orientation with the methoxyl group aiming above the furanose ring. Also, in the case of **3**, MP2 lowers the energy of *gg* compared to B3LYP or even HF. It is known that the MP2 energies are in general very susceptible to the basis set superposition error (BSSE)[64] and the MP2 method very often overestimates the correlation contribution.[65–67] Unlike MP2, common DFT functionals do not fully

include the dispersion interactions, and hence it is tricky to decide which method gives better results. For basis sets used here the BSSE effect is presumably small. Also the intramolecular dispersion effects in compounds **1-6** are assumed to be low because of their small size. Nevertheless, the computations suggest that the van de Waals forces between the methyl group and the ring in *gg* conformation cannot be neglected. This could explain the discrepancies between the B3LYP and MP2 energies, and the methyl group in MP2 optimized geometry being due to the dispersion interaction closer to the ring than in the B3LYP geometry (see bellow). Still, at this point it is difficult to make a general statement about reliability of these two methods. The MP2 probably better describes the intramolecular dispersion in *gg* conformer of **1**, but still could overestimate the correlation. Moreover, the dispersion force between the solvent and the solute, although they may compete with the intramolecular ones, are missing in both approaches. The optical rotation modeling thus could provide a welcome feedback due to its strong dependence on the conformation. The conformer ratios are reflected in the total rotations that can be compared to the experiment.

The energies for compound **3** converge for a smaller basis sets than for **1**: the cc-pVQZ basis set provides almost the same results as the larger cc-pV5Z for **3**, but there is still a significant difference ($\sim$0.3 kJ/mol) between these two levels for **1**. The extrapolated MP2/CBS values are in both cases very close to the cc-pV5Z energies. Based on these results we suggest that at least the cc-pV5Z basis set is necessary for estimations of the conformational populations.

As can be seen in Figure 3, the MP2 and B3LYP *gg* geometries are quite close. The geometry of the furanose ring is practically the same. Only the torsion angle C_2—C_1—O_1—C_{Me} differs by $\sim$4 degrees and it is smaller for the MP2 geometry, in which the methyl group is closer to the ring. The figure also comprises the Boltzmann populations of *gt*, *tg* and *gg* conformers. To separate the influence of the geometry on the conformer energies, populations obtained by MP2 for DFT geometries are also included. As can be seen in Figure 3, the influence of the geometry is limited and the MP2 computations for both geometries give nearly same conformer ratios.

Table 3 summarizes relative conformer energies for compounds **1** and **2** in various solvents. The MP2/CBS energies were also calculated. The population of the *gg* conformer of **1** increases with solvent polarity, unlike for compound **2**. This *gg* minimum of **2** (not stable in vacuum) is in all solvents rather

conformations	B3LYP	MP2*	MP2
gt	66	32	30
tg	0	0	0
gg	33	68	70

Figure 3. The difference between B3LYP and MP2 optimized geometries of **1** (left) and Boltzmann populations (%) of the B3LYP and MP2 conformers. Column MP2* represents the B3LYP optimized conformations and their populations calculated at the MP2/CBS level.

Table 3. Calculated Dependence of the Relative Conformer Energies (kJ/mol) on the Solvent.

	Vacuum		C_6H_6 $\varepsilon = 2.2$	$CHCl_3$ $\varepsilon = 4.9$		EtOH $\varepsilon = 24.6$	DMSO $\varepsilon = 46.7$
	B3LYP	MP2	B3LYP	B3LYP	MP2	B3LYP	B3LYP
Compound **1**							
gt	0.0	0.0	0.0	0.0	0.0	0.0	0.0
tg	12.2	12.5	9.3	7.7	7.4	6.1	6.2
gg	1.7	−1.9	3.4	4.9	1.5	5.8	6.1
Compound **2**							
gt	0.0	0.0	0.0	0.0	0.0	0.0	0.0
tg	15.1	13.4	13.3	12.2	10.1	11.4	11.1
gg	–	–	11.1	9.7	11.3	8.7	8.6

Structures were optimized at the B3LYP/6-311++G**/CPCM level. B3LYP and MP2 stand for the B3LYP/cc-pV5Z energies and MP2/CBS energies, respectively.

high in energy and its populations are similar to those of the *tg* conformer. For other compounds **3–6** only the effect of the experimentally relevant chloroform solvent was explored.

Table 4 summarizes calculated Boltzmann populations for all compounds in vacuum and chloroform. In vacuum, the B3LYP populations of **1** and **3** significantly differ from the MP2 ones. For other compounds both methods give similar results. The transition from vacuum to chloroform causes that the population of **1** *gt* conformer increases for both B3LYP and MP2 methods. The increase of *gt* population is bigger for MP2, so that the difference of the MP2 and B3LYP populations is in chloroform smaller than in vacuum. This is consistent with the aforementioned intramolecular dispersion in *gg* of **1**. Unlike in vacuum, the *gg* conformation is not the most stable for MP2 when combined with a dielectric medium, since the polarization effects prevail against dispersion. For compound **2** population of *tg* increases and that of *gg* decreases for both theoretical levels. As a benchmark we include single point calculations at the CCSD(T)/cc-pVTZ level in the last column of Table 4. The CCSD(T) values closely match the MP2/CBS results. Nevertheless, the basis set used for the coupled cluster calculation is rather small as a larger basis set for this method goes beyond our computational possibilities.

DFT and the Specific Rotation

Table 5 summarizes the calculated and experimental $[\alpha]_{589}$ values for **1–6**. The standard 589 nm wavelength was chosen for the comparison because of the known problems with calculated OR in the vicinity of electronic excitation energies that could be encountered predominantly at lower wavelengths, and because of the availability of experimental data. The calculated results correspond to the weighted average over all B3LYP/6-311++G** minima with the B3LYP and MP2 percentages from Table 4. Chloroform as a solvent was included using the CPCM model. The calculated OR signs mostly agree with experiment, except for **3** where the experimental value is very small. Ste-

phens et al. also reported[27] problems with reproducing small optical rotations which was attributed to limitations of the theoretical approach and experimental errors. Kundrat et al. moreover shown that if the overall optical rotation is determined by a cancellation of large contributions from individual conformers, the relative errors in the energies can lead to comparatively large deviations from the experimental optical rotation.[31] Besides, small optical rotations are difficult to measure accurately. We thus can conclude that only for larger ORs $\{>20 \text{ deg}[dm(g/cm^3)]^{-1}\}$ the anomeric configuration can be satisfactorily determined on the basis of the DFT calculations. Mean average deviation (MAD) of calculated values from the experiment was ~53 $\text{deg}[dm(g/cm^3)]^{-1}$ for the B3LYP functional populations. The error is higher for MP2 populations, because of the error in energy of the *gg* conformer of **1**. Although the compound **1** seems anomalous in the whole series, its exclusion from the comparison does not lead to significant changes in MADs, because the deviations from experiment for the β-L-compounds (**2**, **4**, **6**) are much bigger than those in α-L series. The results for compounds **2–6** obtained with both B3LYP and MP2 populations are similar. The problems of the MP2 method to reproduce experimental results of **1** are somewhat inconsistent with reports of Marchesan et al.[17] The authors concluded that the MP2 seems to perform better than DFT in predicting the energies for various conformers of paraconic acid, leading to a better global OR. Also Kundrat et al. reported on the example of amino acids that the usefulness of DFT is limited by the ability to predict correct

Table 4. Calculated Conformer Ratios, As Obtained from the B3LYP/cc-pV5Z, MP2/CBS, and CCSD(T)/cc-pVTZ Energies.

	Vacuum		$CHCl_3$		
	B3LYP	MP2	B3LYP	MP2	CCSD(T)
Compound **1**					
gt	0.66	0.32	0.84	0.62	0.46
tg	0.00	0.00	0.04	0.03	0.02
gg	0.33	0.68	0.12	0.35	0.53
Compound 2					
gt	1.00	1.00	0.97	0.97	0.97
tg	0.00	0.00	0.01	0.02	0.02
gg	–	–	0.02	0.01	0.01
Compound 3					
gt	0.95	0.86	0.94	0.87	0.88
tg	0.01	0.01	0.05	0.06	0.05
gg	0.05	0.13	0.02	0.07	0.08
Compound **4**					
gt	0.99	0.99	0.95	0.97	0.97
tg	0.00	0.00	0.01	0.01	0.01
gg	0.01	0.01	0.04	0.02	0.02
Compound **5**					
gt	0.97	0.93	0.94	0.89	0.89
tg	0.01	0.01	0.05	0.06	0.05
gg	0.02	0.06	0.01	0.04	0.06
Compound **6**					
gt	0.99	1.00	0.98	0.98	0.98
tg	0.00	0.00	0.01	0.01	0.01
gg	0.01	0.00	0.02	0.01	0.01

Table 5. Experimental and Calculated Specific Rotations {in deg[dm(g/cm^3)]$^{-1}$}.

Compd.	Exp.	Empirical			B3LYP			mB3LYP			CCSD		
		A	B	C	A	B	C	A	B	C	A	B	C
1	−60	−33	−45	−53	−54	3	44	−52	−18	7	−51	−34	−21
2	167	146	146	146	209	210	210	141	141	141	158	159	159
3	−6	−11	−11	−11	42	54	50	14	22	19	−2	5	3
4	106	85	85	85	216	221	222	142	145	146	173	178	179
5	−27	−58	−57	−57	−78	−66	−66	−53	−46	−46	−36	−30	−31
6	155	128	128	128	216	216	216	149	149	149	182	182	183
MAD					53	64	70	20	27	31	21	25	27
MAD′					63	68	76	22	24	21	34	36	39

The rotations are averaged over 3 minima obtained at the DFT/aug-cc-pVDZ level with classical B3LYP functional and its modified mB3LYP version (0.7E_x^{HF}) and at the CCSD/6-31G** level. Empirical values (Emp.) were obtained from the experiment (Exp.) by subtracting the B3LYP/aug-cc-pVDZ vibrational corrections. Boltzmann averaged rotations, as well as vibrational corrections, were calculated from the B3LYP/cc-pV5Z (A) and MP2/CBS (B) and CCSD(T)/cc-pVTZ (C) energies. Both experiment and calculation were performed in CHCl$_3$. MAD is a mean average deviation from experiment, MAD′ is the deviation from corresponding Empirical values.

relative energies and the resulting Boltzmann factors for the accessible geometric conformations.[31,32] A polarizable model as the solvent description seems to work reasonably well, but only in cases where intramolecular hydrogen bonding is not a major factor. When intramolecular hydrogen bonding comes into play, DFT coupled with PCM model tends to estimate the wrong magnitude of the bonding. For better comparison with experiment, the vibrational corrections were subtracted from the experimental values and signed as empirical values (columns 3, 4, 5 in Table 5).

The dependence of OR on the DFT functional is demonstrated for compound **2** in Figure 4. The results were averaged over the three local minima (*gt*, *tg*, *gg*). The hybrid functionals B3LYP and B3PW91 yield substantially smaller deviations from

experiment than the OLYP and PBE GGA functionals. This was also observed for other compounds. However, the simplest HF method provided better results than those from all standard functionals (see Fig. 4). This suggest that the exact exchange energy is particularly important for OR. To further explore its role, we modified the B3LYP functional (containing by definition 20% of the HF term) by increasing the amount of the Hartree-Fock exchange energy (E_X^{HF}) from 10 to 90% with a 10% step and calculated ORs of all *gt* conformers of **1–6**. An amount of 80% was determined as the most favorable. These results are also presented in Table 5, column mB3LYP. To avoid the account for the vibrational effects, vibrational corrections were subtracted from the experimental values before the fitting. With this modified mB3LYP functional the MAD deviation decreases to
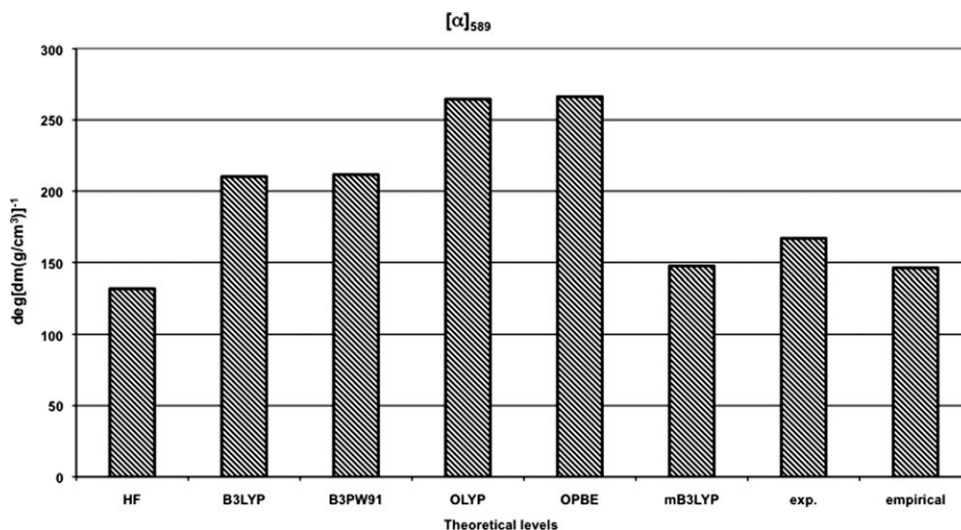
Figure 4. Optical rotation of compound **2** as calculated with different theoretical levels and aug-cc-pVDZ basis set. Displayed [α]$_{589}$ rotations are values averaged over the three B3LYP/6-311++G** local minima. Averaging was based on the B3LYP/cc-pV5Z energies. Empirical values were obtained from the experiment (Exp.) by subtracting the B3LYP/aug-cc-pVDZ vibrational corrections.
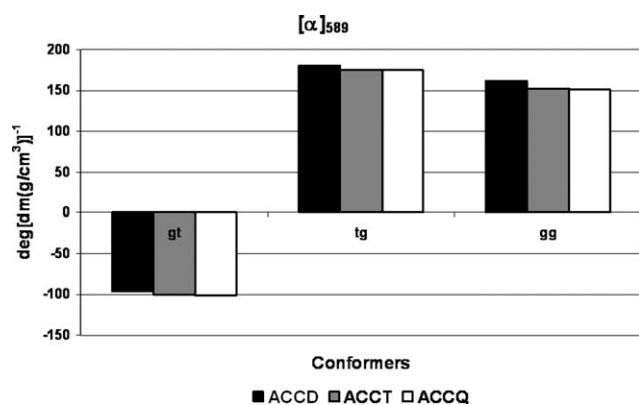
Figure 5. The individual conformer rotations of compound **1** calculated using aug-cc-pVDZ (ACCD), aug-cc-pVTZ (ACCT) and aug-cc-pVQZ (ACCQ) basis sets and the B3LYP functional.

20 and 27 $deg[dm(g/cm^3)]^{-1}$ for the B3LYP populations and MP2 populations, respectively.

Although the B3LYP energies are satisfactory, we see that OR is more sensitive than the energy to the approximations made, and that a higher level of theory is desirable. Hence, the coupled-cluster CCSD method was employed in calculations of $\mathbf{G}'$ for all B3LYP/CPCM minima. Due to computational limits only the 6-31G** basis set was used. The CCSD/6-31G** level gave similar agreement with experiment as our modified mB3LYP functional (c.f. Table 5).

The differences between OR of the *gg* conformer **1** calculated at the B3LYP, mB3LYP, and CCSD could explain the inconsistencies in the MP2 and DFT results. While the DFT functionals gave values between ∼162 and ∼87 $deg[dm(g/cm^3)]^{-1}$, the CCSD value of ∼15 $deg[dm(g/cm^3)]^{-1}$ was substantially smaller. The higher OR and smaller population of *gg* calculated with DFT could have caused a fortuitous error cancellation and a good agreement with experiment. This is seen also in Table 5 if CCSD rotations averaged by MP2 or CCSD(T) energies are compared with empirical values. Deviations from the experiment are similar for all considered approaches and reflect the small basis set used with CCSD, exclusion of triplets in CCSD calculations, and vibrational corrections calculated at the DFT level.

We also tested our mB3LYP functional modification on *S*-methyloxirane which previously served as a convenient benchmark for similar computations.[35,36,68] The mB3LYP/aug-cc-pVTZ gas-phase $[\alpha]_{589}$ value of ∼17.3 $deg[dm(g/cm^3)]^{-1}$ corresponds well to the CC3 value of ∼17.7 $deg[dm(g/cm^3)]^{-1}$ reported by Kongsted et al.,[69] while the standard B3LYP gives the value of about 2 $deg[dm(g/cm^3)]^{-1}$ higher. If the vibrational corrections were included, we obtained $[\alpha]_{589} = -15.5$ $deg[dm(g/cm^3)]^{-1}$ for mB3LYP, which again well agrees with the reported value.[70] Because the gas-phase value at 589 nm is not available, we performed the calculations at 633 nm and 355 nm, for which the experimental values are -8.39 ± 0.2 and $+7.39 \pm 0.30$ $deg[dm(g/cm^3)]^{-1}$, respectively. If we include the Ruud's vibrational corrections[35] in our theoretical values, we obtain the ORs of -6.0 $deg[dm(g/cm^3)]^{-1}$ (633 nm) and 27.6

$deg[dm(g/cm^3)]^{-1}$ (355 nm). Although the results for the lower wavelength are far from experiment, it agrees with previously reported values at the coupled-cluster level.[35]

The increase of the HF exchange in the B3LYP functional thus brought a significant improvement. However, it should be noted that our series of compounds is limited in structural diversity and the convenience of the 80% of HF exchange in B3LYP for OR needs to be verified in the future. For our sugars, we can use it on an empirical basis. More powerful seem to be some advanced techniques; e.g., the optimized-effective potential treatment of the orbital dependent DFT functionals etc.[71]

As was reported before,[25,27,72] the inclusion of the diffuse functions in the basis set is desirable. In our tests a whole set of augmented Dunning type aug-cc-pVnZ ($n = 2, 3, 4$) basis sets was used. Nevertheless, the number of the basis functions had a limited influence on OR (Fig. 5, for compound **1**). The overall rotation changed from -53 $deg[dm(g/cm^3)]^{-1}$ for aug-cc-pVDZ to -58 $deg[dm(g/cm^3)]^{-1}$ for the aug-cc-pVQZ basis.

Frequency Dependence

Figure 6 displays the frequency (wavelength, λ) dependence of ORs for average values over three local minima of **1** obtained at mB3LYP levels with the aug-cc-pVDZ basis set. Note that because of differences in instrumentation, our currently measured experimental value for **1** at 589 nm $\{-60$ $deg[dm(g/cm^3)]^{-1}\}$ is slightly different from that published before $\{-55$ $deg[dm(g/cm^3)]^{-1}\}$.[49] The mB3LYP OR values were calculated for the B3LYP and MP2 populations. The B3LYP populations seem to lead to a better agreement over the whole range of wavelengths if compared to the experiment. Absolute differences between computations and experiment are bigger for smaller λ, but relative differences are similar within the whole range. The absolute value of OR decreases with λ and thus corresponds to the typical relation $\alpha = k/(\lambda^2 - \lambda_0^2)$,[73] where λ_0 is the wavelength of an electronic transition, λ is the wavelength of light and k is a constant. Because the absolute values of optical rotation are bigger for smaller λ, the short wave-
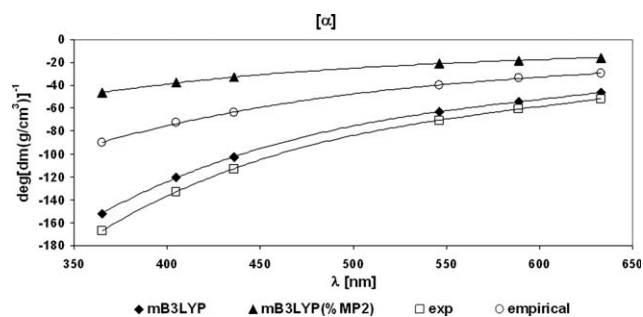
Figure 6. Dependence of the calculated and experimental optical rotation of **1** on the wavelength. The calculations were performed with the modified mB3LYP functional and aug-cc-pVDZ basis with the B3LYP/cc-pV5Z averaging (mB3LYP), or with the MP2/CBS averaging [mB3LYP(%MP2)]. Empirical values were obtained from the experiment (exp.) by subtracting the B3LYP/aug-cc-pVDZ vibrational corrections calculated for all different wavelengths.
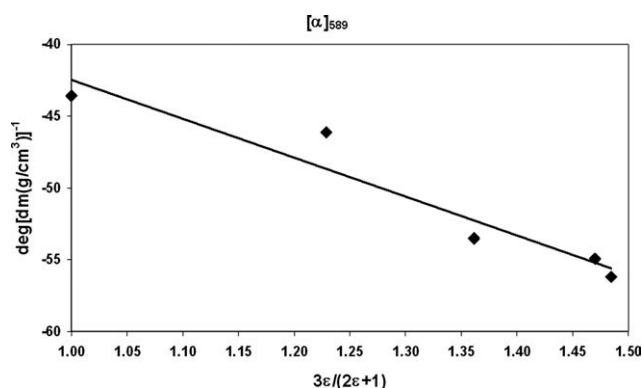
Figure 7. Dependence of the optical rotation of **1** on the solvent Lorentz polarization factor. Calculated rotations (mB3LYP/aug-cc-pVDZ) are based on the B3LYP/cc-pV5Z populations.

length results seem to be more suitable for a comparison with the experiment. However, as pointed before a good agreement between the experiment and mB3LYP predictions with B3LYP averaging can be sometimes fortuitous. Especially for low λ a large error can stem from an inaccurate description of the electronic transitions. Moreover, if vibrational corrections are taken into account within the empirical values, the MP2 averaging seems to provide more reasonable results.

Solvent Effect

The solvent can influence the geometry and energy, as well as the optical tensor itself. In fact, geometrical changes are rather small. However, the energies are in some cases influenced significantly (Table 4). For example, the MP2 populations of **1** and **3** in chloroform are closer to the B3LYP values then in vacuum. As pointed earlier, unlike vacuum some intermolecular interactions can be overcome by polarization effects if a dielectric medium is involved.

The OR solvent effect was estimated at the mB3LYP/aug-cc-pVDZ level for all compounds **1–6**. Figure 7 displays the B3LYP/cc-pV5Z average $[\alpha]_{589}$ values calculated in four solvents and in vacuum. The solvents are characterized by the Lorentz polarization factor $[3\varepsilon/(2\varepsilon + 1)]$ dependent on the electric permittivity ε. As apparent from the figure, the increase of the solvent polarity is accompanied by a nearly linear decrease of the electronic component of OR. Kongsted et al. found an opposite trend for *S*-methyloxirane; however, highly polar solvents (e.g., water) were not investigated because of the limited ability of the dielectric model to distinguish between systems of high dielectric constants.[36]

For all compounds chloroform causes similar changes in rotation {cca 10–20 deg[dm(g/cm^3)]$^{-1}$} as compared to vacuum. In relative terms, the change goes from very large (up to 50% for **3**) to small (<10% for **2, 4, 6**) values. Even though the continuum model in some literature cases did not adequately describe the influence of a solvent, a more accurate explicit model currently goes beyond our computational capabilities.

Vibrational Averaging

Molecular response to the electromagnetic field also includes the nuclear contribution.[34–36,74] We estimated the vibrational parts of OR at the B3LYP/aug-cc-pVDZ level. Vibrational wavefunctions reflecting the cubic and semidiagonal quartic perturbations were employed to assess the effect of anharmonicity. A test calculation on *S*-methyloxirane provided a similar vibrational corrections {~2 deg[dm(g/cm^3)]$^{-1}$, aug-cc-pVDZ basis} as reported previously.[35] Figure 8 summarizes the vibrational changes of optical rotations of **1–6** caused by the first and
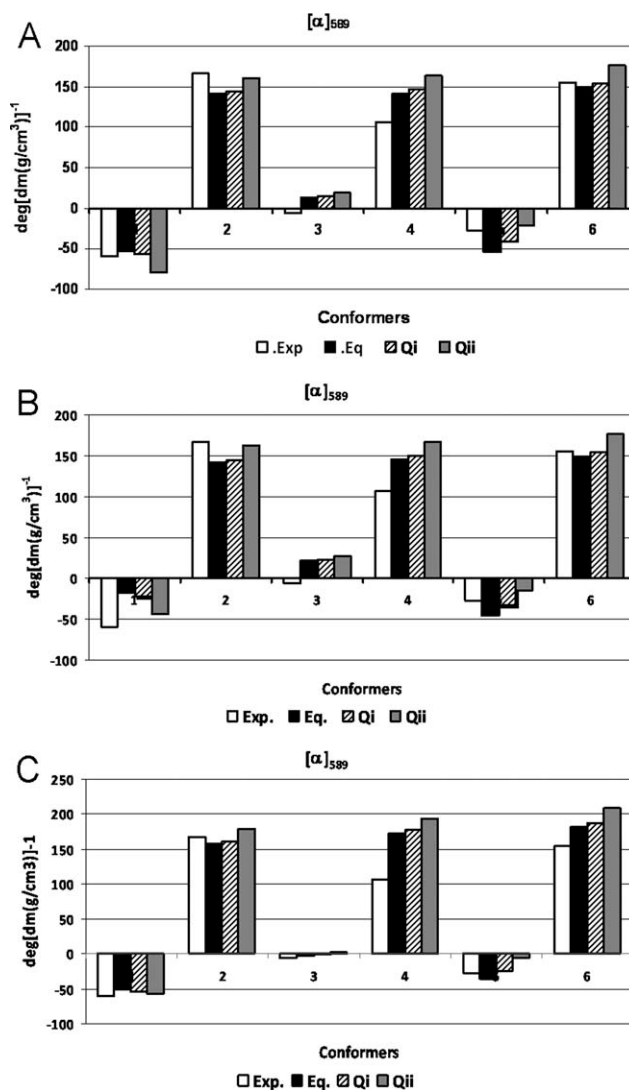
Figure 8. Optical rotations of compounds **1-6** calculated with the zero (equilibrium), first (Qi), and second (Qii) OR derivative corrections (obtained at the at the B3LYP/aug-cc-pVDZ level) as compared to the experiment. Top and middle parts display mB3LYP/aug-cc-pVDZ equilibrium rotations averaged with B3LYP/cc-pV5Z (A) and MP2/CBS energies (B), respectively. Bottom panel represent CCSD/6-31G** equilibrium values averaged with CCSD(T)/cc-pVTZ energies (C).
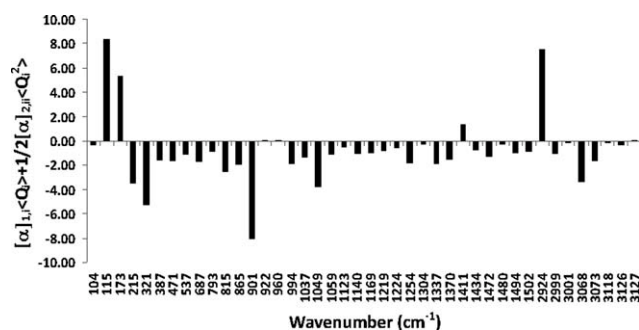
Figure 9. Contributions of individual normal modes to the OR vibrational correction in the methyl 2,3-anhydro-L-erythrofuranoside (**1**) in *gg* conformation.

second property derivatives. Overall rotations, as well as vibrational corrections, were averaged over all local minima with B3LYP/cc-pV5Z and MP2/CBS populations, respectively. The mB3LYP/aug-cc-pVDZ equilibrium values were used. Chloroform was included via the CPCM model. Moreover, the influence of vibrations can be assessed from Table 5, where the empirical columns represent experimental values minus vibrational corrections (first and diagonal second derivatives). The inclusion of vibrational correction causes for all methods an increase of absolute value of OR for all compounds, except for **5**. Vibrational averaging does not change the signs of OR. The contribution of the OR first derivatives is almost negligible {$\sim$4 deg[dm(g/cm^3)]$^{-1}$}, especially if we realize the error of the experiment {$\sim$20 deg[dm(g/cm^3)]$^{-1}$}, and its involvement results in the same mean average deviations as for the equilibrium values. On the other hand, the second derivatives cause an average change of about $\sim$15 deg[dm(g/cm^3)]$^{-1}$, but do not improve the overall agreement with experiment {for example MAD = 22 deg[dm(g/cm^3)]$^{-1}$ for mB3LYP and B3LYP/cc-pV5Z averaging}, which was already pointed out by Mort and Autschbach.[74] Only for **2** and **5** the vibrational averaged values are better. Note, that if the MP2 averaging is used, vibrations cause a better agreement with experiment also in **1**.

Similar deviations are obtained if the CCSD equilibrium values are used together with the DFT vibrational parts, exploring the additivity (perturbational character) of the corrections.[35,37] In compound **3** the corrections caused a sign change. For compound **1** the vibrations slightly improved the agreement with experiment. It is, however, difficult to separate the role of the vibrational corrections from the total error as, for example, the MP2 energies used for the averaging of mB3LYP rotations instead of DFT caused similar changes. In the light of the vibrational contribution it looks like the good agreement based on the DFT energy averaging was fortuitous and MP2/CBS or CCSD(T)/cc-pVTZ give more reasonable conformational fractions. Further improvement could be expected if both higher theoretical method (coupled-cluster) and basis sets (at least aug-cc-pVTZ) were employed, which is, unfortunately, beyond current computational possibilities. The used computational methods are most probably too inaccurate to benefit from the vibrational averaging.

To better understand the role of individual vibrations in the averaging, in Figure 9 we plot the relative values of the approximate vibrational contributions of individual modes, $[\alpha]_{1,i} < Q_i > + \frac{1}{2}[\alpha]_{2,ii} < Q_i^2 >$ [cf. eq. (6)]. As apparent from the figure, all harmonic normal modes contribute to the rotation. The contributions of the first three lowest-energy modes cannot be considered reliable as these modes (e.g., methyl rotation and methoxy bending) exhibit a strongly anharmonic potential, for which the limited Taylor expansion [eq. (5)] is most probably inappropriate. Hopefully, the Boltzmann averaging of the lowest-energy conformers accounted or compensated for part of their vibrational contribution, as these modes are associated with the conformer transitions. The other two most-contributing modes involve the furanose ring breathing (901 cm^{-1}) and the C—H stretching (2924 cm^{-1}) at the furanose carbon bearing the methoxyl group. No rule of thumb to predict the biggest contributions thus comes to our mind, and a complete estimation of the corrections for all the modes seems as the only option. In particular, the relatively weak contribution of the C—H stretching modes (except for the 2924 cm^{-1} stretch) is rather surprising as they are strongly anharmonic in the energy surface.[46] Similarly as for NMR,[37] the mid IR modes ($\sim$300–1600 cm^{-1}) seem to contribute more in total.

Despite all, the vibrational corrections are an important factor necessary for computing optical rotations. Autschbach et al. reported that while most of the correction occurs at the zero-point level, the inclusion of temperature effects in the vibrational averaging can elucidate the temperature-dependence of the optical rotation from a purely vibrational effect.[31] They concluded that the temperature dependence of the OR is a result of the intrinsic temperature-dependent vibrational corrections. Moreover, it should be noted that vibrational corrections for systems with methyl groups could be contaminated by methyl rotations at higher temperatures.[32] Such advanced vibrational calculations could be combined with solvent models to obtain more accurate calculations of OR, especially in rigid organic molecules where there is little interaction between the solvent and the molecules of interest, and would be included in our future works.

Conclusions

On a series of conformationally restricted saccharide derivatives we investigated the optical rotation calculations as a qualitative tool for the conformational space evaluation. The potential energy surface of studied compounds was explored at several DFT and wavefunction [MP2 and CCSD(T)] levels. On the basis of the relative conformer energies the Boltzmann populations were estimated. The population fractions were then combined with the optical rotations calculated for all conformers. The TDDFT and CCSD methods were tested for the calculation of OR. The influence of the solvent, frequency dependence, and vibrational contributions were included and discussed.

All theoretical levels described the PESs of most studied compounds similarly. For **1** the B3LYP method gave a very different conformer relative energies and populations than the MP2 or CCSD(T) levels. Among the DFT functionals only the hybrid ones provided good optical rotations. The results were further

improved by increasing the amount of the HF exchange in the classical B3LYP functional from 20 to 80%, which resulted in a very low error {MAD $\sim$20 deg[dm(g/cm^3)]$^{-1}$}. Similar deviations were obtained with the much more computationally expensive CCSD method. Increasing the size of the basis set beyond aug-cc-pVDZ had a limited effect on OR. The vibrational averaging improved results in two cases only; most probably, the computational methods used were too inaccurate to profit from it. This aspect will be addressed in a separate study in the future. The changes in the geometry caused by the solvents were negligible; however, chloroform modeled with CPCM significantly influenced the vacuum optical rotation values, energy and conformer populations.

Overall, the optical rotation appears as a welcome probe in the modeling of flexible compounds. Several computational bottlenecks have to be watched carefully: The Boltzmann populations exponentially depend on rather inaccurate conformer energies. Standard DFT functionals do not accurately reproduce van der Waals dispersions and the electronic excitation energies required for the dynamical (frequency-dependent) optical rotation tensor. The solvent influences geometries, energies, and optical rotations, and thus should be included at least as a continuum model. The vibrational averaging is recommended in general, but may not improve inaccurate equilibrium OR values. However, the vibrational contribution induces the change in overall optical rotation and thus the good agreement of the equilibrium OR based on the DFT energy averaging was fortuitous and MP2/CBS or CCSD(T) appears to give more reasonable conformational fractions.

Acknowledgments

References

1. Huryn, D. M.; Okabe, M. Chem Rev 1992, 92 1745.
2. Habich, D.; Barth, W. Synthesis 1988, 943.
3. Mengel, R.; Griesser, H. Tetrahedron Lett 1977, 18 1177.
4. Suhodalnik, R. J. Nucleoside Antibiotics; Wiley Interscience: New York, 1970.
5. Goodman, L.; Christensen, J. E. J Am Chem Soc 1961, 83, 3823.
6. Balzarini, J.; Pauwels, R.; Baba, M.; Robins, M. J.; Zou, R.; Herdewijn, P.; De Clerq, E. Biochem Biophys Res Commun 1987, 145, 269.
7. Datema, R.; Remaud, G.; Bazin, H.; Chattopadhyaya, J. Biochem Pharm 1983, 38, 109.
8. Lin, T. S.; Chen, M. S.; McLaren, C.; Gao, Y.-S.; Prusoff, W. H. J Med Chem 1987, 30, 440.
9. Krayevsky, A. A.; Kukhanova, M. A.; Atrazhev, A. M.; Dyatkina, N. B.; Papchibin, A. V.; Chidgeavadze, Z. G.; Beabcalashvilli, R. S. Nucleosides Nucleotides 1988, 7, 613.
10. Edward., J. T. Chem Ind 1955, 1102.
11. Runtz, G.; Bader, R. F. W.; Messer, R. R. Can J Chem 1977, 55, 3040.
12. Kaminsky, J.; Raich, I. J Mol Struct: THEOCHEM 2008, 860, 32.
13. Bouř, P.; Raich, I.; Kaminský, J.; Hrabal, R.; Čejka, J.; Sychrovský, V. J Phys Chem A 2004, 108, 6365.
14. Polavarapu, P. L.; Chakraborty, D. K.; Ruud, K. Chem Phys Lett 2000, 319, 595.
15. Pecul, M.; Ruud, K.; Rizzo, A.; Helgaker, T. J Phys Chem A 2004, 108, 4269.
16. Kondru, R. K.; Wipf, P.; Beratan, D. N. J Phys Chem A 1999, 103, 6603.
17. Marchesan, D.; Coriani, S.; Forzato, C.; Nitti, P.; Pitacco, G.; Ruud, K. J Phys Chem A 2005, 109, 1449.
18. Amos, R. D. Chem Phys Lett 1982, 87, 23.
19. Polavarapu, P. L. Mol Phys 1997, 91, 551.
20. Helgaker, T.; Ruud, K.; Bak, K. L.; Joergensen, P.; Olsen, J. Faraday Discuss 1994, 99, 165.
21. Polavarapu, P. L.; Chakraborty, D. K. Chem Phys 1999, 240, 1.
22. Kondru, R. K.; Wipf, P.; Beratan, D. N. J Am Chem Soc 1998, 120, 2204.
23. Polavarapu, P. L.; Petrovic, A.; Wang, F. Chirality 2003, 15, S143.
24. Wiberg, K. B.; Vaccaro, P. H.; Cheeseman, J. R. J Am Chem Soc 2003, 125, 1888.
25. Cheeseman, J. R.; Frisch, M. J.; Devlin, F. J.; Stephens, P. J. J Phys Chem A 2000, 104, 1039.
26. Grimme, S.; Furche, F.; Ahlrichs, R. Chem Phys Lett 2002, 361, 321.
27. Stephens, P. J.; Devlin, F. J.; Cheeseman, J. R.; Frisch, M. J. J Phys Chem A 2001, 105, 5356.
28. Sadlej, A. J. Coll Czech Chem Commun 1988, 53, 1995.
29. Autschbach, J.; Ziegler, T. J Chem Phys 2002, 116, 891.
30. Ruud, K.; Helgaker, T. Chem Phys Lett 2002, 352, 533.
31. Kundrat, M. D.; Autschbach, J. J Phys Chem A 2006, 110, 4115.
32. Kundrat, M. D.; Autschbach, J. J Phys Chem A 2006, 110, 12908.
33. Ruud, K.; Stephens, P. J.; Devlin, F. J.; Taylor, P. R.; Cheeseman, J. R.; Frisch, M. J. Chem Phys Lett 2003, 373, 606.
34. Pedersen, T. B.; Kongsted, J.; Crawford, T. D.; Ruud, K. J Chem Phys 2009, 130, 034310.
35. Ruud, K.; Zanasi, R. Angew Chem Int Edit 2005, 44, 3594.
36. Kongsted, J.; Ruud, K. Chem Phys Lett 2008, 451, 226.
37. Dračínský, M.; Kaminsky, J.; Bouř, P. J Chem Phys 2009, 130, 094106.
38. Mennucci, B.; Tomasi, J.; Cammi, R.; Cheeseman, J. R.; Frisch, M. J.; Devlin, F. J.; Stephens, P. J. J Phys Chem A 2002, 106, 6102.
39. Stephens, P. J.; Devlin, F. J.; Cheeseman, J. R.; Frisch, M. J.; Mennucci, B.; Tomasi, J. Tetrahedron Asymmetry 2000, 11, 2443.
40. Kundrat, M. D.; Autschbach, J. J Chem Theory Comput 2008, 4, 1902.
41. Goldsmith, M. R.; Jayasuria, N.; Beratan, D. N.; Wipf, P. J Am Chem Soc 2003, 125, 15696.
42. Mukhopadhyay, P.; Wipf, P.; Beratan, D. N. Acc Chem Res 2009, 42, 809.
43. Mukhopadhyay, P.; Zuber, G.; Goldsmith, M. R.; Wipf, P.; Beratan, D. N. Chem Phys Chem 2006, 7, 2483.
44. Dračínský, M.; Kaminský, J.; Bouř, P. J Phys Chem B 2009, 113, 14698.
45. Rosenfeld, L. Z Phys 1928, 52, 161.
46. Daněček, P.; Bouř, P. J Comput Chem 2007, 28, 1617.
47. Bouř, P. S4 program, Academy of Sciences: Prague, 1994–2009.
48. Jarý, J.; Raich, I. Carbohydr Res 1993, 242, 291.
49. Raich, I. PhD Thesis, VŠCHT, Praha, 1994.
50. Schejter, A.; George, P. Biochemistry 1964, 3, 1045.
51. Altona, C.; Sundaralingam, M. J Am Chem Soc 1972, 94, 8205.
52. Karton, A.; Martin, J. M. L. Theor Chem Acc 2006, 115, 330.
53. Helgaker, T.; Klopper, W.; Koch, H.; Noga, J. J Chem Phys 1997, 106, 9639.
54. Barone, V.; Cossi, M. J Phys Chem A 1998, 102, 1995.
55. Handy, N. C.; Cohen, A. J. Mol Phys 2001, 99, 403.

56. Lee, C.; Yang, W.; Parr, R. G. Phys Rev B 1988, 37, 785.
57. Perdew, J. P.; Burke, K.; Ernzerhof, M. Phys Rev Lett 1996, 77, 3865.
58. Becke, A. Phys Rev A 1988, 38, 3098.
59. Perdew, J. P.; Chevary, J. A.; Vosko, S. H.; Jackson, K. A.; Pederson, M. R.; Singh, D. J.; Fiolhais, C. Phys Rev B 1992, 46, 6671.
60. Frisch, M. J.; Trucks, G. W.; Schlegel, H. B.; Scuseria, G. E.; Robb, M. A.; Cheeseman, J. R.; Montgomery, J. J. A.; Vreven, T.; Kudin, K. N.; Burant, J. C.; Millam, J. M.; Iyengar, S. S.; Tomasi, J.; Barone, V.; Mennucci, B.; Cossi, M.; Scalmani, G.; Rega, N.; Petersson, G. A.; Nakatsuji, H.; Hada, M.; Ehara, M.; Toyota, K.; Fukuda, R.; Hasegawa, J.; Ishida, M.; Nakajima, T.; Honda, Y.; Kitao, O.; Nakai, H.; Klene, M.; Li, X.; Knox, J. E.; Hratchian, H. P.; Cross, J. B.; Bakken, V.; Adamo, C.; Jaramillo, J.; Gomperts, R.; Stratmann, R. E.; Yazyev, O.; Austin, A. J.; Cammi, R.; Pomelli, C.; Ochterski, J. W.; Ayala, P. Y.; Morokuma, K.; Voth, G. A.; Salvador, P.; Dannenberg, J. J.; Zakrzewski, V. G.; Dapprich, S.; Daniels, A. D.; Strain, M. C.; Farkas, O.; Malick, D. K.; Rabuck, A. D.; Raghavachari, K.; Foresman, J. B.; Ortiz, J. V.; Cui, Q.; Baboul, A. G.; Clifford, S.; Cioslowski, J.; Stefanov, B. B.; Liu, G.; Liashenko, A.; Piskorz, P.; Komaromi, I.; Martin, R. L.; Fox, D. J.; Keith, T.; Al-Laham, M. A.; Peng, C. Y.; Nanayakkara, A.; Challacombe, M.; Gill, P. M. W.; Johnson, B.; Chen, W.; Wong, M. W.; Gonzalez, C.; Pople, J. A. Gaussian 03, Gaussian, Inc.: Wallingford, CT, 2004.
61. Angeli, C.; Bak, K. L.; Bakken, V.; Christiansen, O.; Cimiraglia, R.; Coriani, S.; Dahle, P.; Dalskov, E. K.; Enevoldsen, T.; Fernandez, B.; Haettig, C.; Hald K.; Halkier, A.; Heiberg, H.; Helgaker, T.; Hettema, H.; Jensen, H. J. A.; Jonsson, D.; Joergensen, P.; Kirpekar, S.; Klopper, W.; Kobayashi, R.; Koch, H.; Lutnaes, O. B.; Mikkelsen, K. V.; Norman, P.; Olsen, J.; Packer, M. J.; Pedersen, T. B.; Rinkevicius, Z.; Rudberg, E.; Ruden, T. A.; Ruud, K.; Salek, P.; Sanchez de Meras, A.; Saue, T.; Sauer, S. P. A.; Schimmelpfennig, B.; Sylvester-Hvid, K. O.; Taylor, P. R.; Vahtras, O.; Wilson, D. J.; Agren, H. DALTON, a molecular electronic structure program, Release 2.0, University of Oslo: Oslo, 2005.
62. Haasnoot, C. A. G.; de Leeuw, F. A. A. M.; Altona, C. Tetrahedron 1980, 36, 2783.
63. Kaminsky, J.; Jensen, F. J Chem Theor Comput 2007, 3, 1774.
64. Kaminsky, J.; Mata, R. A.; Werner, H.-J.; Jensen, F. Mol Phys 2008, 106, 1899.
65. van Mourik, T.; Karamertzanis, P. G.; Price, S. L. J Phys Chem A 2006, 110, 8.
66. van Mourik, T.; Holfroyd, L. F. Chem Phys Lett 2007, 442, 42.
67. Shields, A.; van Mourik, T. J Phys Chem A 2007, 111, 13272.
68. Crawford, T. D.; Tam, M. C.; Abrams, M. L. J Phys Chem A 2007, 111, 12057.
69. Kongsted, J.; Pedersen, T. B.; Strange, M.; Osted, A.; Hansen, A. E.; Mikkelsen, K. V.; Pawlowski, F.; Jørgensen, P.; Hättig, C. Chem Phys Lett 2005, 401, 385.
70. Wilson, S. M.; Wiberg, K. B.; Cheeseman, J. R.; Frisch, M. J.; Vaccaro, P. H. J Phys Chem A 2005, 109, 11752.
71. Lutnæs, O. B.; Teale, A. M.; Helgaker, T.; Tozer, D. J.; Ruud, K.; Gauss, J. J Chem Phys 2009, 131, 144104.
72. Pecul, M.; Ruud, K.; Helgaker, T. Chem Phys Lett 2004, 388, 110.
73. Polavarapu, P. L. Chirality 2002, 14, 768.
74. Mort, B. C.; Autschbach, J. J Phys Chem A 2005, 109, 8617.